

Original Article

# Simulation of Optimal Photovoltaic Energy Injection into an Unstable Grid: Case Study in Burkina Faso

Kiswēndsida Philippe KOUANDA<sup>1</sup>, Seydou Ouedraogo<sup>1,2</sup>, Ousmane Nikiema<sup>1</sup>, Adekunlé Akim Salami<sup>1</sup>

<sup>1</sup>Regional Centre of Excellence for Electricity Management, University of Lomé, Lomé, Togo.

<sup>2</sup>Department of Electrical Engineering, University Institute of Technology, Nazi Boni University, Bobo-Dioulasso, Burkina Faso.

<sup>2</sup>Corresponding Author: oseydou2@gmail.com

Received: 12 August 2025

Revised: 15 September 2025

Accepted: 18 October 2025

Published: 30 October 2025

**Abstract** - To optimise the integration of photovoltaic electricity into an unstable power grid, it is necessary to find the appropriate location and optimal power of the photovoltaic electricity to be injected into the power grid. The method used consists of varying the photovoltaic power to be injected at the optimal point until an overload of one or more elements of the grid is observed. The modelling of the electricity grid and the simulation of the injection of photovoltaic power into the grid are carried out using NEPLAN software. For this study, the injection points of the Zagtoui, Komsilga, and Kossodo stations of the national interconnected grid (RIN), as seen from Ouagadougou, were selected. The simulation results gave an optimal photovoltaic power of 70 MW at the Zagtoui station, 100 MW at the Kossodo station, and 70 MW at the Komsilga station. The results obtained in this study can be used to optimise the integration of photovoltaic power plants into the national interconnected grid of Burkina Faso and into the national grids of West African countries based on their similarities.

**Keywords** - Photovoltaic Power, Electricity, Grid, Unstable, Injection, Optimisation.

## 1. Introduction

In recent years, demand for electricity in West African countries has been steadily increasing, mainly due to demographic changes and the development of certain urban areas. This problem is exacerbated by the unprecedented instability of the grids, which are plagued by power cuts and load shedding. To meet this exorbitant demand for energy, power plants in these developing countries must rise to the challenge. Like the rest of the world, these countries use fossil fuels such as coal, oil, gas, and uranium to generate electricity. With the gradual depletion of global reserves of these conventional energy sources and, above all, the global warming caused by their use, renewable energies are seen as an alternative for electricity generation [1].

Thus, due to the enormous potential of solar energy in this sub-region, the establishment and integration of photovoltaic power plants into national grids is being prioritised in order to tackle the energy crisis. To this end, a number of gigantic solar photovoltaic power plants have been built, feeding into the public electricity grids. Examples include the 33 MWp photovoltaic power plant in Zagtoui, Ouagadougou, Burkina Faso, the 6.5 MWp photovoltaic power plant in Praia, Cape Verde [2], and the 50 MWp power plant in the city of Blitta, Togo. Large-scale photovoltaic electricity injection projects are also being considered to improve access to electrical

energy [3]. The increase in photovoltaic installations poses the challenge of integrating them into existing grids [4, 5]. The challenge of feeding photovoltaic electricity into public grids lies not only in their optimised management, but above all in their impact in terms of disruption to these grids [6]. The main problem associated with connecting photovoltaic generators to the public electricity grid is that it can have various adverse effects on the operation of the photovoltaic power plants themselves and on the electricity grid [7].

In order to meet the requirements guaranteeing the capabilities of the distribution grid in terms of voltage stability, power loss reduction, reliability, and cost-effectiveness, in short, energy quality, the optimal integration of photovoltaic generators is essential [8, 9]. The location and size of photovoltaic power plants play an important role in the operation and planning of electricity grids [10].

Suboptimal integration of photovoltaic power plants can have adverse effects on the electricity grid [23, 24]. This study, based on an analytical approach due to the complexity of innovative technologies, does not take into account the protection devices of the grid under study, which may be the subject of another study, but focuses on the optimal integration of PV energy into a grid that is sometimes disrupted by outages and load shedding. This article aims to determine the



optimal power output of PV power plants to be injected simultaneously into the three substations studied, taking into account grid constraints. It is structured as follows: 2. Literature review, followed by a presentation of the study grid in the third part. The fourth part is devoted to the equipment and methodology, the fifth part to the results and discussion, and finally the sixth part to the conclusion.

## 2. Literature Review

Researchers in research studies have developed methods to determine the optimal location for photovoltaic power plants and the appropriate amount of power to be injected [13]. In the presence of decentralised generators, with their locations predetermined (nodes 7, 10, and 30), Dulau et al. (2015) presented a technique based on Optimal Power Flow (OPF) calculation with a view to minimising fuel costs and joule losses [14].

In a 2005 study, Momoh et al. used the Continuous Power Flow (CPF) method and the voltage stability index to decide which node to place photovoltaic power plants on, based on where the voltage is degraded, in order to decide which node to target (candidate nodes) [15].

In order to demonstrate the influence of photovoltaic power plants on greenhouse gas emissions and fuel costs, L. Yingchen et al. (2010) used the optimisation technique based on the interior point method in their study, with the location of the photovoltaic power plants being chosen in advance [16]. Y. Zhu et al. (2007), with a view to minimising total network losses, formulated the Optimal Power Flow (OPF) in the distribution network in the presence of photovoltaic power plants using the quadratic programming method for resolution [17]. Harrison et al. (2022) developed a method based on OPF in the distribution network with photovoltaic power plants considered as negative loads [18].

In order to solve the Optimal Power Flow (OPF) problem, the distributed and Parallel OPF (DPOPF) algorithm was proposed by Lin et al. (2013) in the presence of photovoltaic power plants in the transmission network [19].

Other authors have presented the Particle Swarm Optimisation (PSO) technique to determine the optimal location and size of different types of photovoltaic power plants in distribution networks [20]. In order to determine the optimal location and size of photovoltaic power plants, Masoud (2013) proposed a multi-objective optimisation (minimisation of active losses and number of photovoltaic power plants) based on the non-linear programming technique [21]. A hybrid method combining Genetic Algorithms (GA) and PSO was presented by Moradi et al. (2012) with a view to determining the optimal location of photovoltaic power plants in a distribution network with different objective functions, such as improving the voltage profile, the voltage stability

margin, and minimizing losses [22]. Mohammadi et al. used a multi-objective approach to define the optimal location and power to be injected into the distribution network using the NSGA-II (Non-dominated Sorting Genetic Algorithms II) method [23].

In the search for the best location and adequate power to inject with the objective function of minimising active losses in the network, Benyagoub et al. (2018) studied the optimal decentralised integration of sources based on genetic algorithms subject to technical and safety constraints [24].

In the literature, studies focusing on the optimal integration of decentralised generators are widely discussed. This integration is much more relevant to distribution networks. It reveals, through the various methods used, that the electrical parameters of these networks are impacted when the number of connected decentralised sources becomes significant. If these sources are introduced in an optimal manner in terms of size and location, they considerably reduce active losses in the network.

In Burkina Faso, located in West Africa, where this study is being conducted, the electricity supply is provided by thermal power plants, hydroelectric power plants, and electricity imports from neighbouring countries, Côte d'Ivoire and Ghana. Burkina Faso aims to inject nearly 650 MW into its electricity grid by 2030.

Currently, electricity from three photovoltaic power plants is fed into the interconnected national grid: the Zagtouli photovoltaic power plant, with a maximum capacity of 33 MW, the Ziga photovoltaic power plant, with a maximum capacity of 1.1 MW, and the Nagréongo plant, with a maximum capacity of 26 MW, representing a total capacity of 60.1 MW currently injected, which is only about 9% of the planned capacity. This study focuses on optimising the simultaneous injection of photovoltaic electricity at the injection points of three substations of the RNI in Burkina Faso, located in West Africa.

The main objective of this study is to determine the maximum power of photovoltaic electricity that can be injected simultaneously at the injection points of the Zagtouli, Kossodo, and Komsilga stations of the Ouagadougou network without causing a major failure across the entire RNI.

## 3. Presentation of the Grid

The electrical network covered by this study is the National Interconnected Network (RNI) as seen from Ouagadougou, the capital of Burkina Faso, a West African country. The location of the photovoltaic energy injection points on this interconnected network has been chosen in advance. The electrical diagram of the Ouagadougou city grid, with the injection points, is shown in Figure 1.

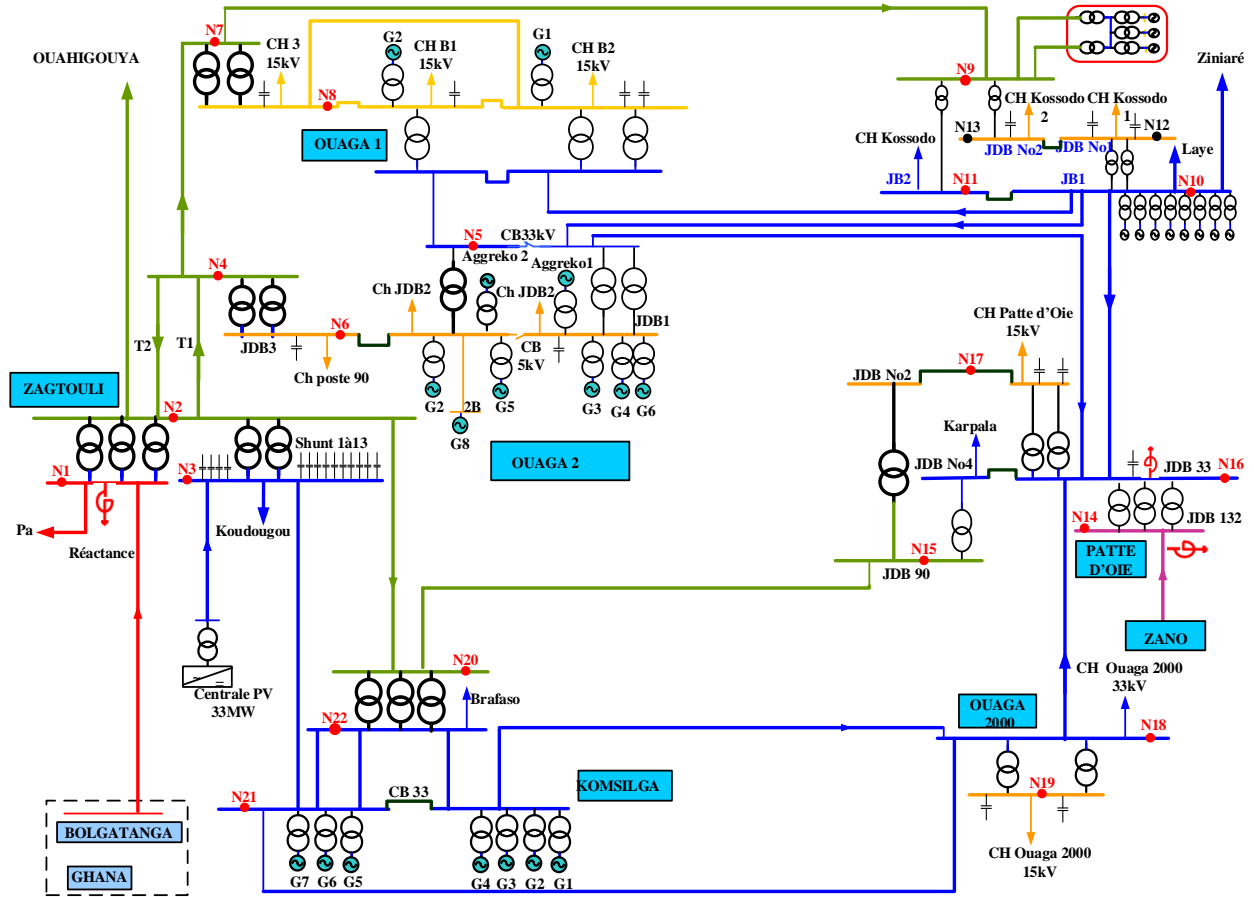


Fig. 1 Single-line diagram of the grid as seen from Ouagadougou

The RNI, as seen from Ouagadougou, consists of seven (07) power stations, namely: Zagtouli, Komsilga, Ouaga 1, Ouaga 2, Kossodo, Patte d'Oie, and Ouaga 2000. In addition to being interconnection stations, Ouaga 1, Ouaga 2, Kossodo, and Komsilga are thermal power stations, while Zagtouli has a photovoltaic power station and two 225 kV lines from Côte d'Ivoire and Ghana.

The Zagtouli station has three buses: 225 kV, 90 kV, and 33 kV. It has three nodes: N1, N2, and N3.

The Ouaga 2 station has three buses: 90 kV, 33 kV, and 15 kV. It has three nodes: N4, N5, and N6.

The Ouaga 1 station has two buses: 90 kV and 15 kV. It has two nodes: N7 and N8.

The Kossodo station has five buses: one 90 kV bus, two 33 kV buses, and two 15 kV buses. It has five nodes: N9, N10, N11, N12, and N13.

The Patte d'Oie station has four busbars: 132 kV, 33 kV, and two 15 kV. It has four nodes: N14, N15, N16, and N17.

The Ouaga 2000 station has two sets of busbars, 33 kV and 15 kV. It has two nodes: N18 and N19.

The Komsilga station has three voltage levels: 90 kV, 33 kV, and 15 kV. It has three nodes: N20, N21, and N22.

Energy is exchanged with the rest of the country via the Zagtouli, Patte d'Oie, and Kossodo substations.

#### 4. Equipment and Method

This study aims to determine the optimal power output from photovoltaic power plants to be fed simultaneously into the Zagtouli, Kossodo, and Komsilga stations. The decision variables are the maximum photovoltaic power to be injected into the Zagtouli, Kossodo, and Komsilga stations, taking into account grid constraints [25, 26].

The methodology consists of simultaneously varying the photovoltaic power to be injected at the injection point of the Zagtouli, Kossodo, and Komsilga stations up to the convergence or overload limit of a network element (transformer, line, nodes, etc.). The constraints associated with optimising injection are such that the voltage and frequency of the grid must remain within contractual limits, the total energy in the lines must be at most equal to their capacity, and the power supplied by the generators and transformers must be within nominal limits.

This study will not focus solely on the maximum capacity of the injection point, but will also highlight the impact of this injection on the network, in particular, the voltage variation and the contribution of the balancing node, i.e., the interconnection with Ghana.

#### 4.1. Grid Modelling

The network modelling takes into account loads, transformers, generators, lines, and buses [27]. First, an inventory must be made of the equipment of the interconnected network loads and those of the loads connected to this interconnected network, as seen from the city of Ouagadougou. Then the powers connected to the nodes must be aggregated.

Active elements are modelled using their subtransient reactance. For power distribution, these elements are modelled by their active and reactive powers or by the amplitude and angle of the voltage of the designated node [28].

The data collected across the entire network will be used to determine the power connected to each node in the network.

The active power connected to a node is calculated by:

$$P_i = \sum_{j=1}^m (\sum_{k=1}^n P_k) k_{uk} k_{sk} \quad (1)$$

Where  $P_i$  = the active power connected to node  $i$ ,  $P_k$ ,  $k_{uk}$ ,  $k_{sk}$  = respectively the power, utilisation factor, and simultaneity factor of household  $k$ ,  $m$  = the number of plots connected to the node,  $n$  = the number of households in plot  $j$ .

The reactive power connected to node  $i$  is calculated using the following formula:

$$Q_i = P_i \tan \varphi \quad (2)$$

Where  $P_i$  = the active power connected to node  $i$ ,  $Q_i$  = the reactive power connected to node  $i$ , and  $\varphi$  = the phase shift.

The lines are characterised by their type, length, current capacity, linear resistance, linear reactance, and linear capacitance.

Transformers are defined by their apparent power, iron losses, primary voltage, secondary voltage, and short-circuit voltage. Once the network model seen from Ouagadougou has been obtained, it is essential to check the validity of the model.

#### 4.2. Formulation of the Photovoltaic Injection Optimisation Problem Photovoltaic Injection

The calculation method used in this study is *Newton-Raphson's* method. Proposed by *Isaac Newton* and *Joseph Raphson*, it is an iterative method widely used to solve non-linear equations [29, 30]. An admittance matrix is used to

write the equations for the currents in the nodes of the electrical network, expressed in polar coordinates, where  $j$  includes the node  $i$ .

$$I_i = \sum_{j=1, i=1}^n |Y_{ij}| |V_i| < \theta_{ij} + \delta_j \quad (3)$$

Where  $I_i$  = current in node  $i$ ,  $Y_{ij}$  = admittance of branch  $ij$ ,  $V_i$  = voltage of node  $i$ ,  $\theta_{ij}$  = phase shift of branch  $ij$ ,  $\delta_j$  = voltage angle of node  $i$ .

The active and reactive powers at node  $i$  are given by:

$$P_i - jQ_i = V^* I_i \quad (4)$$

Where  $P_i$  and  $Q_i$  = active and reactive power at node  $i$ , respectively,  $V_i$  = voltage at node  $i$ ,  $I_i$  = current in node  $i$ .

Substituting  $I_i$  from Equation (3) into Equation (4), we obtain:

$$P_i - jQ_i = |V_i| < -\delta_j \sum_{j=1, i=1}^n |Y_{ij}| |V_i| < \theta_{ij} + \delta_j \quad (5)$$

The real and imaginary parts are separated as follows:

$$P_i = \sum_{j=1, i=1}^n |Y_{ij}| |V_i| |V_j| \cos(\theta_{ij} - \delta_i + \delta_j) \quad (6)$$

$$Q_i = \sum_{j=1, i=1}^n |Y_{ij}| |V_i| |V_j| \sin(\theta_{ij} - \delta_i + \delta_j) \quad (7)$$

The elements of the Jacobian matrix are obtained after partial derivation of Equations (6) and (7). The equation can be written in matrix form, given that:

$$\begin{bmatrix} \Delta P \\ \Delta Q \end{bmatrix} = \begin{bmatrix} J_1 & J_3 \\ J_2 & J_4 \end{bmatrix} \begin{bmatrix} \Delta \delta \\ \Delta V \end{bmatrix} \quad (8)$$

Where  $J_1$ ,  $J_2$ ,  $J_3$ , and  $J_4$  = the elements of the Jacobian matrix.

The corrected values of iteration  $k$  can be expressed by the deviations ( $\Delta P_i^{(k)}$  and  $\Delta Q_i^{(k)}$ ), which are represented as follows:

$$\Delta P_i^{(k)} = P_i^{sp} - P_i^{(k)cal} \quad (9)$$

$$\Delta Q_i^{(k)} = Q_i^{sp} - Q_i^{(k)cal} \quad (10)$$

Where  $P_i^{sp}$  and  $Q_i^{sp}$  = the specified values  $P_i$  and  $Q_i$  at node  $i$ .  $P_i^{(k)cal}$  and  $Q_i^{(k)cal}$  = the calculated values  $k^{th}$  iteration.

The new estimated values of the node voltage are given by relations (11) and (12):

$$\delta_i^{(k+1)} = \delta_i^{(k)} + \Delta \delta_i^k \quad (11)$$

$$|V^{(k+1)}| = |V_i^{(k)}| + \Delta|V_i^{(k)}| \quad (12)$$

This research aims to determine the optimal power to be injected by the photovoltaic power plant, which minimises active losses while taking into account grid constraints. To do this, it is necessary to define the fitness function and the equality and inequality constraints.

Various objective functions are taken into account, namely the minimisation of active losses, the maximisation of the voltage stability index, the improvement of the voltage profile, the minimisation of greenhouse gases, etc. [31]. In this study, the objective is also to minimise active losses at the line level. The minimisation of these losses is expressed as:

$$\min [P_{active}^T] = \min \sum_{i=1}^{N_B} r_i I_i^2 \quad (13)$$

Where  $r_i$  and  $I_i$  = respectively, the resistance and current in the power line,  $N_B$  = the number of branches,  $P_{active}^T$  = the total active losses of the network.

The function expressing active losses is subject to a set of equality and inequality constraints that must be satisfied while minimizing active losses. The equality constraints represent the power balance equations between generation and consumption for a transmission network with photovoltaic installations.

The active and reactive power equality constraints can be expressed as:

$$\begin{cases} \sum_{i=1}^{N_G} P_{G_i} + \sum_{i=1}^{N_{CPV}} P_{CPV_i} - \sum_{i=1}^{N_L} P_{D_i} - \sum_{i=1}^{N_B} P_{loss_i} = 0 \\ \sum_{i=1}^{N_G} Q_{G_i} + \sum_{i=1}^{N_{CPV}} Q_{CPV_i} - \sum_{i=1}^{N_L} Q_{D_i} - \sum_{i=1}^{N_B} Q_{loss_i} = 0 \end{cases} \quad (14)$$

Where  $P_G$  and  $Q_G$  = the active and reactive power of the conventional generator,  $P_{CPV}$  and  $Q_{CPV}$  = the active and reactive power supplied by the photovoltaic power plants,  $P_D$  and  $Q_D$  = the active and reactive power of the load node,  $P_{loss}$  and  $Q_{loss}$  = the active and reactive power losses,  $N_L$ ,  $N_G$ ,  $N_B$  and  $N_{CPV}$  = the number of load nodes, the number of generators, the number of branches and the number of photovoltaic power plants. The inequality constraints represent the physical limits of the lines, conventional generators, and photovoltaic power plants, as well as the safety limits of the voltages at the network nodes. The power limits of the photovoltaic power plants are given by:

$$P_{CPV_i}^{min} \leq P_{CPV_i} \leq P_{CPV_i}^{max}, \forall i \in [1, N_{CPV}] \quad (15)$$

Where  $P_{CPV_i}^{min}$  = the minimum active power limit generated by the photovoltaic power plant at the JB busbar  $i$ ,  $P_{CPV_i}^{max}$  = the maximum active power limit generated by the photovoltaic

power plant at the JB busbar  $i$ ,  $N_{CPV}$  = the set of indices of all generator busbars. In order to maintain the quality of the electrical service and the safety of the system, it is necessary to limit violations of voltage constraints, which must remain within their permissible limits according to:

$$V_i^{min} \leq V_i \leq V_i^{max}, \forall i \in N \quad (16)$$

Where  $V_i^{min}$  = the minimum limit of the voltage module at the JB busbar  $i$ ,  $V_i^{max}$  = the maximum limit of the voltage module at the JB busbar  $i$ ,  $N$  = the number of buses in the system.

For reasons of electrical grid safety, the penetration rate of photovoltaic installations in the grid is set at a limit based on the robustness of the grid [32, 33]. The penetration rate is given by:

$$r_p = \frac{\sum_{i=1}^{N_{CPV}} P_{CPV_i}}{\sum_{i=1}^{N_L} P_{D_i}} \times 100 \quad (17)$$

Where  $P_{CPV}$  = the total active power of the photovoltaic installations,  $P_{D_i}$  = the total active power demanded or the total power produced by conventional sources.

During the optimisation process, we may encounter unfeasible solutions due to exceeding the voltage constraint or the thermal limit of the lines. In this case, we penalise the objective function [34, 35]. It is then reformulated as:

$$OF = \sum_{i=1}^{N_B} r_i I_i^2 + k_p (P_{G_i} - P_{G_i}^{lim})^2 + k_Q \sum_{i=1}^{N_G} (Q_{G_i} - Q_{G_i}^{lim})^2 + k_V \sum_{i=1}^{N_L} (V_{L_i} - V_{L_i}^{lim})^2 + k_S \sum_{i=1}^{N_B} (S_{B_i} - S_{B_i}^{lim})^2 \quad (18)$$

With:

$$V_{L_i}^{lim} = \begin{cases} V_{L_i}^{max}, si V_{L_i} > V_{L_i}^{max} \\ V_{L_i}^{min}, si V_{L_i} < V_{L_i}^{min} \\ V_{L_i}, si V_{L_i}^{min} \leq V_{L_i} \leq V_{L_i}^{max} \end{cases} \quad (19)$$

And:

$$S_{L_i}^{lim} = \begin{cases} V_{b_i}^{max}, si S_{b_i} > S_{b_i}^{max} \\ S_{L_i}^{min}, si S_{b_i} < S_{b_i}^{min} \\ S_{L_i}, si S_{b_i}^{min} \leq S_{b_i} \leq S_{b_i}^{max} \end{cases} \quad (20)$$

Where  $k_p$ ,  $k_Q$ ,  $k_V$ , and  $k_S$  = respectively the penalty constants for the active and reactive power produced by the reference generator (voltage bus), the voltage at the load nodes, and the penalty constant for the thermal limit of the lines,  $r_i$  and  $I_i$  = respectively the resistance and current in the power line.

The problem can therefore be summarised as a constrained optimisation problem, which can be formulated as follows:

$$\begin{cases} \min(FO) \\ \text{Contraintes} \end{cases} \quad (21)$$

#### 4.3. Troubleshooting Injection Optimisation

Injection optimisation consists of determining the maximum power to be injected at the injection points, beyond which serious disturbances can occur on the electrical network. The diagram in Figure 2 shows the steps involved in optimising the photovoltaic power to be injected at each

station. There are several simulation tools in the form of software or simulators for distribution and/or transmission networks. Real-time simulators include OPAL-RT Technology, HyperSim, etc. [36]. Existing software includes static and/or dynamic real-time and offline simulation software [37]. Offline simulation software includes EUROSTAG, Power System Simulator for Engineering (PSS/E), dig silent Power Factory (Digital Simulation and Electrical Networks), NEPLAN, etc. NEPLAN software is a tool used in planning and information systems for electricity, gas, water supply, and heating networks [38]. All the basic components of the electrical network in NEPLAN are shown in the structure in Figure 3.

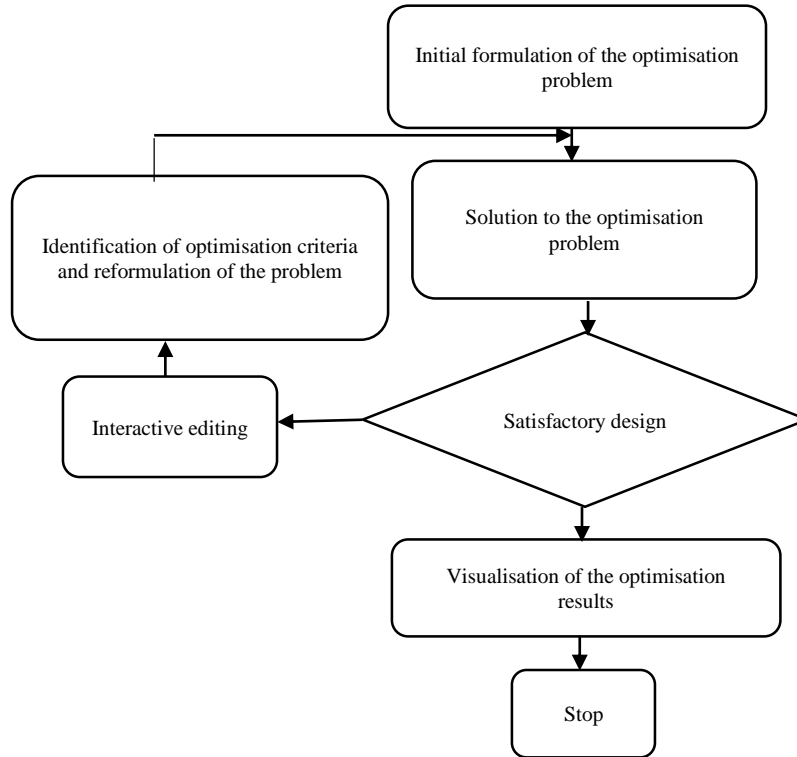


Fig. 2 Algorithm for solving the photovoltaic power optimisation problem

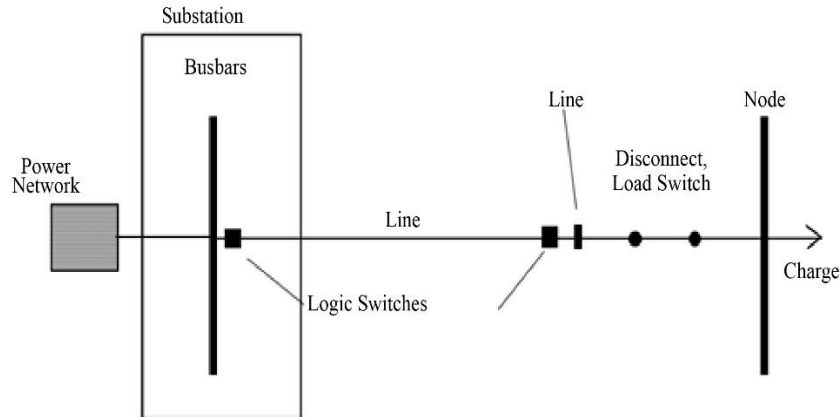


Fig. 3 Representation of network components in NEPLAN

The maximum photovoltaic power to be injected into these stations, taking into account network constraints, is sought. NEPLAN software, which is free for up to 50 nodes and meets pre-established criteria, is used. The parameters are entered into NEPLAN using a data entry mask.

## 5. Results and Discussions

The sites covered by this study are the Zagtouli, Kossodo, and Komsilga stations, all located in the city of Ouagadougou. Network modelling and photovoltaic injection simulation are carried out using version 5 of the NEPLAN software.

### 5.1. National Interconnected Network Model

Figure 4 shows the structure of the interconnected electricity network model as seen from the city of Ouagadougou.

There are twenty-two (22) nodes. Points designated P1 to P7 (Figure 4) are the various measurement points that will be used to validate the model. To validate the network model, its characteristics will be compared with those of the distribution system.

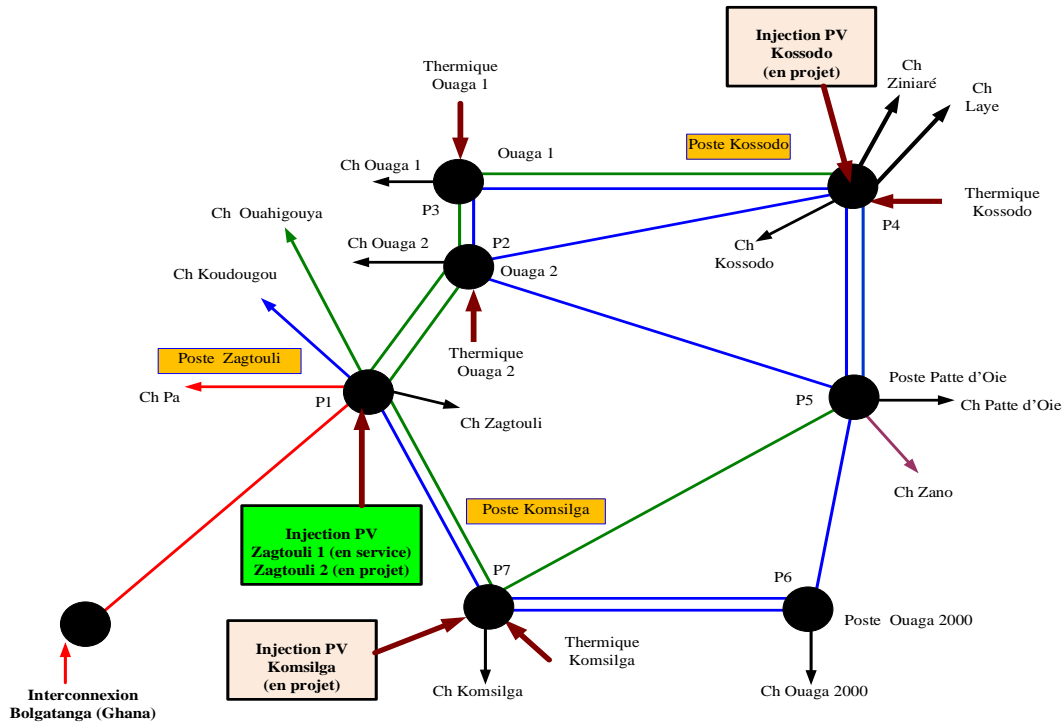


Fig. 4 Structure of the network model as seen from the city of Ouagadougou

Table 1 gives the voltage values of the distribution nodes across the entire network of the city of Ouagadougou.

Table 1. Node voltage values

Station	Node	Designation	Nominal voltage (kV)	Distribution voltage (kV)	Model voltage (kV)
Zagtouli	N1	Busbar sets_225kV_Zagtouli	225	226.27	223.91
	N2	Busbar assemblies_90 kV_Zagtouli	90	94.02	92.268
	N3	Busbar assemblies_33 kV_Zagtouli	33	34.53	34.56
Ouaga2	N4	Busbar assemblies_90kV_Ouaga2	90	92.67	91.37
	N5	Busbar assemblies_33 kV_Ouaga2	33	32.75	33.30
	N6	Busbar assemblies_15 kV_Ouaga2	15	15.64	15.28
Ouaga1	N7	Busbar assemblies_90kV_Ouaga1	90	92.45	91.15
	N8	Busbar assemblies_15 kV_Ouaga1	15	15.52	15.20
Kossodo	N9	Busbar assemblies_90kV_Kossodo	90	91.92	90.74
	N10	Busbar assemblies_33 kV_Kossodo	33	32.11	33.16
	N11	Busbar assemblies_33kV_Kossodo	33	32.90	33.17
	N12	Busbar sets_15kV_Kossodo	15	15.66	15.12

	N13	Busbar assemblies_15 kV_Kossodo	15	15.67	14.98
<b>Goose foot</b>	N14	Busbar assemblies _132kV_Patte d'Oie	132	131.89	132.86
	N15	Busbar assemblies _90 kV Patte d'Oie	90	92.21	91.11
	N16	Busbar assemblies _33 kV Patte d'Oie	33	32.21	32.32
	N17	1_15 kV busbar assemblies_Patte d'Oie	15	15.34	14.67
<b>Ouaga2000</b>	N18	33kV busbar assemblies Ouaga 2000	33	32.59	32.11
	N19	Busbar assemblies_15 kV_ Ouaga2000	15	15.29	15.16
<b>Komsilga</b>	N20	Busbar assemblies _90kV_Komsilga	90	93.62	92.09
	N21	Busbar assemblies_33 kV_Komsilga	33	33.55	33.85
	N22	Busbar assemblies_33kV_Komsilga	33	33.5	33.84

The results of the model simulations and the distribution characteristics are shown in Figure 5. For the distribution system, the maximum variation in node voltage relative to their nominal values is 104.60%, while the minimum variation is 98.80%. For the model, the maximum variation in node

voltage relative to their nominal values is 104.73%, while the minimum variation is 97.29%. The node voltage values for the distribution and the model are similar for all stations. Figure 6 shows the difference between the variation in the voltage of the distribution nodes and that of the model.

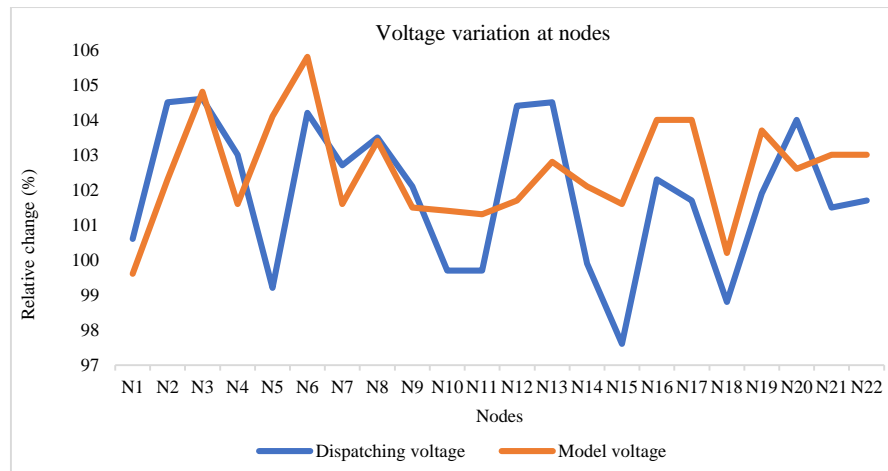


Fig. 5 Relative voltage variation curve of the nodes

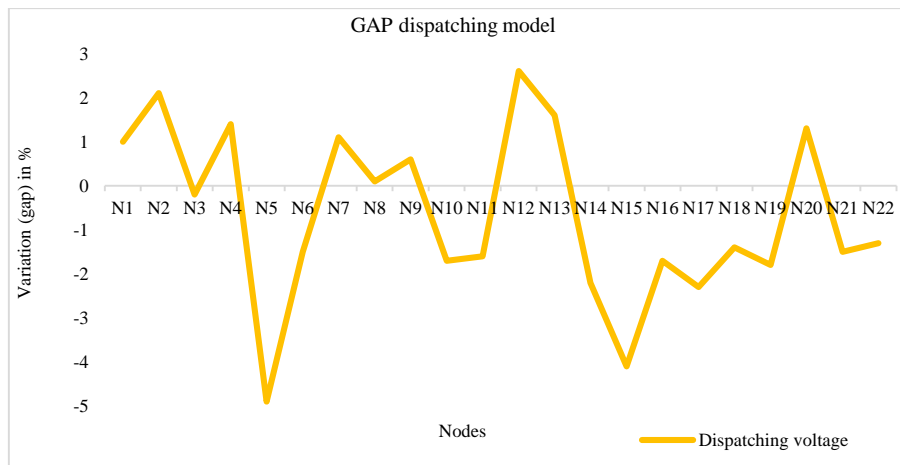


Fig. 6 Curve showing the difference in node voltage variation



The maximum relative difference between the model values and those of the distribution is 4.9% on node 5. The minimum variation of 0.1% is observed on node 8. As this variation is below the imposed limit of 10%, the model therefore reflects the reality of the national electricity grid as seen from Ouagadougou.

## 5.2. Results of the Photovoltaic Injection Simulation

The limit constraints set for voltage variation in the stations must not exceed 120% of the nominal voltage of each station, and the current in the lines must not exceed the nominal current of each line. The results of the simulations of

simultaneous photovoltaic electricity injection at the Zagtouli, Kossodo, and Komsilga stations are presented below.

### 5.2.1. Voltage Variation in Stations

Figure 7 shows the voltage variation curves in the stations as a function of the power simultaneously injected into the Zagtouli, Kossodo, and Komsilga stations.

It can be seen that above 60 MW at the Zagtouli station, 110 MW at the Kossodo station, and 70 MW at Komsilga, the voltage variation at the various stations exceeds the authorised limit.

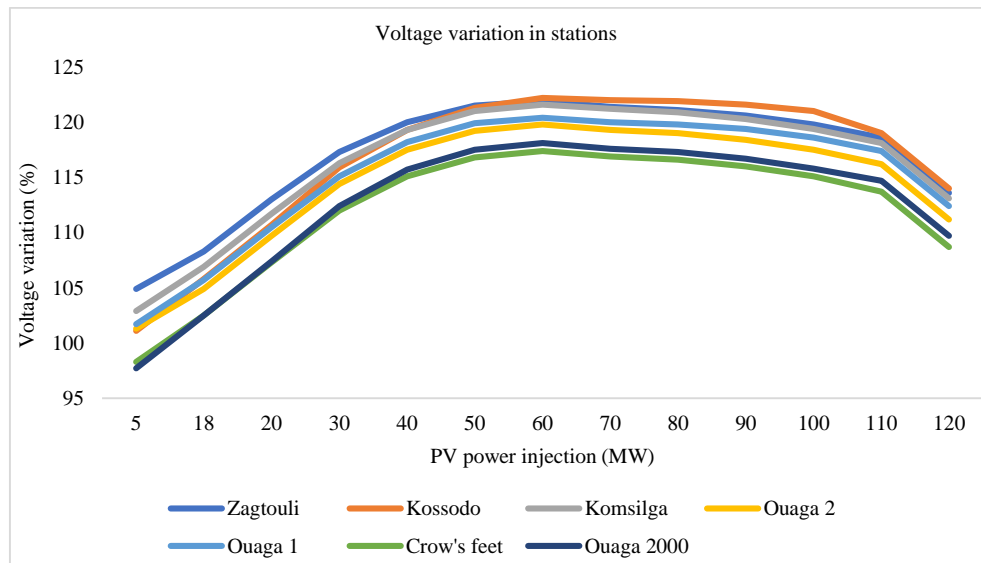


Fig. 7 Voltage variations in the stations

The photovoltaic power injected simultaneously at the Zagtouli, Kossodo, and Komsilga stations causes a voltage variation in the network of between 97.7% and 119.9% of the nominal voltage, i.e., an increase of 19.9% of the nominal voltage (Un).

The maximum photovoltaic power fed into the grid simultaneously is therefore 60 MW at the Zagtouli station, 110 MW at the Kossodo station, and 70 MW at the Komsilga station.

In accordance with the technical constraints associated with grid operation, the simultaneous injection of photovoltaic energy at the Zagtouli, Kossodo, and Komsilga stations requires voltage regulation at each injection point and the appropriate placement of production sources in other regions.

### 5.2.2. Variation in Line Current

Table 2 shows the variation in current on the line connecting Zagtouli to Komsilga. It can be seen that above 60 MW at the Zagtouli station, 110 MW at the Kossodo station, and 70 MW at the Komsilga station, the line connecting the Zagtouli station to the Komsilga station is overloaded.

Table 2. Line current values

Photovoltaic energy is injected at the station			90 kV line
Zagtouli (MW)	Kossodo (MW)	Komsilga (MW)	Current value (A)
5	5	5	168.2
18	18	18	105.0
20	20	20	100.4
30	30	30	114.1
40	40	40	152.7
50	50	50	199.7
60	60	60	250.9
60	70	70	305.7
60	80	70	319.5
60	90	70	333.7
60	100	70	348.4
60	110	70	364.2
<b>70</b>	<b>120</b>	<b>80</b>	<b>440.8</b>

If the photovoltaic power injected reaches 70 MW at the Zagtouli station, 120 MW at the Kossodo station, and 80 MW at the Komsilga station (Table 2), the 90 kV line from the

Zagtouli station to the Komsilga station would carry a current of 440.8 A, or a load of 120.8% compared to the nominal current of 365 A. Figure 8 shows the evolution of the current on the line between the Zagtouli station and the Komsilga station. The line current decreases during the simultaneous injection of photovoltaic energy between 5 and 20 MW. The current increases rapidly when the injected power is between 20 MW and 70 MW. Between 70 MW and 110 MW of

injected photovoltaic power, the increase in current is moderate. Above 110 MW, the line current exceeds the nominal current of 365 A. Above 110 MW of photovoltaic power, the line is overloaded and injection is no longer possible. This confirms that the optimal photovoltaic power that can be injected simultaneously into these three stations is 60 MW at the Zagtouli station, 110 MW at the Kossodo station, and 70 MW at the Komsilga station.

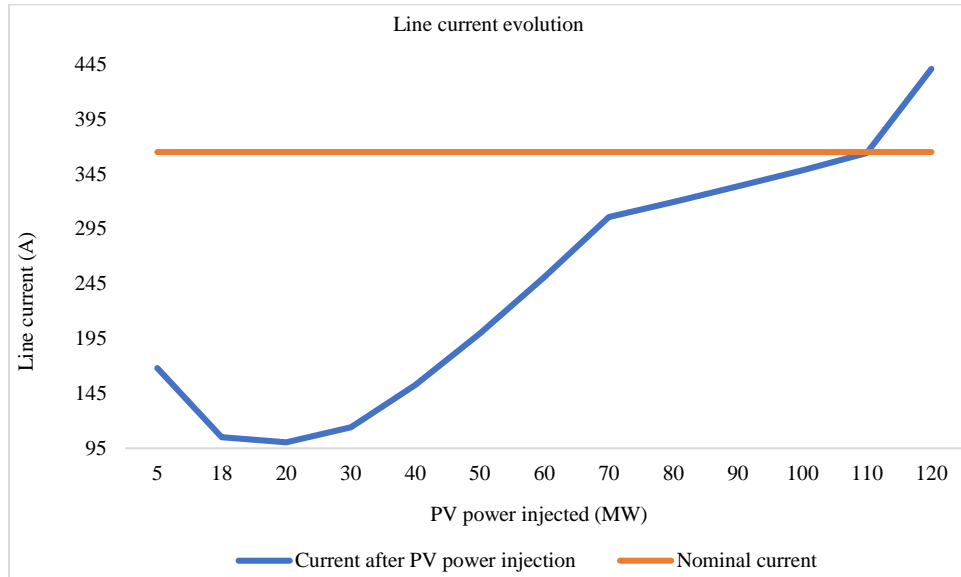


Fig. 8 Evolution of line current

### 5.2.3. Behaviour of the Interconnection with Ghana

The Behaviour of the interconnection line with Ghana (Figure 4) in terms of power flow is shown in Table 3. In fact, above 180 MW (60 MW x 3) (Table 3), there is a significant return of active power to Ghana. When photovoltaic injection

exceeds 60 MW at the Zagtouli station, 110 MW at the Kossodo station, and 70 MW at the Komsilga station, respectively, active power of up to 77 MW returns to Ghana via the interconnection line. This results in a significant loss of the supply of the interconnected national electricity grid.

Table 3. Variations in active and reactive power on the interconnection line

Photovoltaic power injected at the station			Interconnection with Ghana	
Zagtouli (MW)	Kossodo (MW)	Komsilga (MW)	Active power (MW)	Reactive power (MVar)
5	5	5	-145,409	3,565
18	18	18	-106,591	24,039
20	20	20	-100,626	26.00
30	30	30	-70,966	39,034
40	40	40	-41,287	46,818
50	50	50	-11,561	49,800
<b>60</b>	<b>60</b>	<b>60</b>	<b>18,210</b>	<b>48,471</b>
60	70	70	38,000	44,367
60	80	70	47,886	42,216
60	90	70	57,737	38,968
60	100	70	67,558	34,475
60	110	70	77,344	28,480
70	120	80	107,111	3,842

### 5.3. Power Losses in the Grid

The total power produced by the grid (photovoltaic, thermal, etc.) is 432 MW, while the power consumed in the

grid is 420 MW. Losses in the grid are estimated at 12 MW, or 3% of the total power consumed. These losses are relatively low.

#### 5.4. Penetration Rate

The maximum photovoltaic power injected into the electricity grid as seen from the city of Ouagadougou is 240 MW. The power absorbed by the RNI as seen from Ouagadougou is 163 MW.

The permissible penetration rates are 47% in 2022 and 31% in 2030 for the grid seen from Ouagadougou. For the entire RNI, the rates are 36% and 23%. The grid seen from the city of Ouagadougou represents 75% of the NIG and has a capacity of 38%. Of all solar photovoltaic projects in the country.

#### 5.5. Comparison of Results

Comparing the results of the study with the literature, there is a similarity in the contribution of PV generators to minimising active losses in the network. This reduction in

losses becomes significant in most case studies in the literature when at least four decentralised sources are integrated, whereas in the present study, with three injection points, it is estimated at 12 MW.

#### 6. Conclusion

This study highlighted the limit of the photovoltaic power to be injected and its impact on the grid, in particular, the voltage variation between 102.9% and 122.2% and the contribution of the balancing node, which represents the compensation power for the intermittency of photovoltaic production. In cases where interconnections provide this compensation, it is necessary to provide an equivalent power reserve to support the grid in the event of an interconnection failure. The results obtained will provide decision-makers and stakeholders with an optimised analysis tool for the injection of energy from renewable sources into the grid.

#### References

- [1] M. Bissiri et al., "Towards a Renewable Energy Future for West African States: A Review of Electricity System Planning Approaches," *Renewable and Sustainable Energy Reviews*, vol. 134, 2020. [[CrossRef](#)] [[Publisher Link](#)]
- [2] Daniel Vázquez Pombo et al., "The Islands of Cape Verde as a Reference System for 100% Renewable Deployment," *2021 IEEE Green Technologies Conference (GreenTech)*, Denver, CO, USA, pp. 455-461, 2021. [[CrossRef](#)] [[Google Scholar](#)] [[Publisher Link](#)]
- [3] Bo Zhao et al., "Network Partition-Based Zonal Voltage Control for Distribution Networks with Distributed PV Systems," *IEEE Transactions on Smart Grid*, vol. 9, no. 5, pp. 4087-4098, 2018. [[CrossRef](#)] [[Google Scholar](#)] [[Publisher Link](#)]
- [4] Elizabeth L. Ratnam, Steven R. Weller, and Christopher M. Kellett, "Scheduling Residential Battery Storage with Solar PV: Assessing the Benefits of Net Metering," *Applied Energy*, vol. 155, pp. 881-891, 2015. [[CrossRef](#)] [[Google Scholar](#)] [[Publisher Link](#)]
- [5] Amar Hadj Arab et al., "Voltage Quality at the Injection Point of the CDER Photovoltaic System," *Journal of Renewable Energies - CDER*, vol. 20, no. 1, pp. 1-9, 2017. [[CrossRef](#)] [[Publisher Link](#)]
- [6] Marco Cavana et al., "Electrical and Gas Networks Coupling through Hydrogen Blending under Increasing Distributed Photovoltaic Generation," *Applied Energy*, vol. 290, 2021. [[CrossRef](#)] [[Google Scholar](#)] [[Publisher Link](#)]
- [7] Md Shafiullah, Shakir D. Ahmed, and Fahad A. Al-Sulaiman, "Grid Integration Challenges and Solution Strategies for Solar PV Systems: A Review," *IEEE Access*, vol. 10, pp. 52233-52257, 2022. [[CrossRef](#)] [[Google Scholar](#)] [[Publisher Link](#)]
- [8] Talada Appala Naidu, Sajan K. Sadanandan, and Tareg Ghaoud, "Power Quality in Grid-Connected PV Systems: Impacts, Sources, and Mitigation Strategies," *IEEE Smart Grid Bulletin*, 2021. [[Google Scholar](#)] [[Publisher Link](#)]
- [9] Luis M. Castro, J.R. Rodríguez-Rodríguez, and Cecilia Martín-del-Campo, "Modelling Photovoltaic Systems as Distributed Energy Resources for Steady-State Power Flow Studies," *International Journal of Electrical Power and Energy Systems*, vol. 115, pp. 1-9, 2020. [[CrossRef](#)] [[Google Scholar](#)] [[Publisher Link](#)]
- [10] G. Maliki et al., "Analysis of the Impacts of Increased Penetration of Electrical Grids by Photovoltaic Generators," *Maghrebien Journal of Pure and Applied Science*, vol. 8, no. 2, pp. 111-121, 2022. [[CrossRef](#)] [[Publisher Link](#)]
- [11] Bilal Taghezouit et al., "Model-Based Fault Detection in Photovoltaic Systems: A Comprehensive Review and Avenues for Enhancement," *Results in Engineering*, vol. 21, pp. 1-23, 2024. [[CrossRef](#)] [[Google Scholar](#)] [[Publisher Link](#)]
- [12] Akshay Narendra Deshmukh, and VK Chandrakar, "Power Quality Issues and Mitigation Techniques in Grid-Connected Solar Photovoltaic Systems - A Review," *2021 International Conference on Computer Communication and Informatics (ICCCI)*, Coimbatore, India, pp. 1-6, 2021. [[CrossRef](#)] [[Google Scholar](#)] [[Publisher Link](#)]
- [13] J.A. Peças Lopes et al., "Integration of Distributed Generation into Electric Power Systems: A Review of Drivers, Challenges, and Opportunities," *Electric Power Systems Research*, vol. 77, no. 9, pp. 1189-1203, 2007. [[CrossRef](#)] [[Google Scholar](#)] [[Publisher Link](#)]
- [14] Lucian-Ioan Dulău, Mihail Abrudean, and Dorin Bică, "Optimal Power Flow Analysis of a Distributed Generation System," *Procidia Technology*, vol. 19, pp. 673-680, 2015. [[CrossRef](#)] [[Google Scholar](#)] [[Publisher Link](#)]
- [15] James Momoh, and Garfield D. Boswell, "Value-Based Implementation of Distributed Generation in Optimal Power Flow," *Proceedings of the 37<sup>th</sup> Annual North American Power Symposium*, Ames, IA, USA, pp. 27-33, 2005. [[CrossRef](#)] [[Google Scholar](#)] [[Publisher Link](#)]
- [16] Yingchen Liao et al., "Notice of Retraction: Optimal Power Flow of Receiving Power Network Considering Distributed Generation and Environment Pollution," *2010 Asia-Pacific Power and Energy Engineering Conference*, Chengdu, China, 2010. [[CrossRef](#)] [[Google Scholar](#)] [[Publisher Link](#)]

- [17] Y. Zhu, and K. Tomsovic, "Optimal Power Flow for Systems with Distributed Energy Resources," *Electric Power Energy Systems*, vol. 29, no. 3, pp. 260-267, 2007. [[CrossRef](#)] [[Google Scholar](#)] [[Publisher Link](#)]
- [18] Rahul Ranjan Jha et al., "Distribution Grid Optimal Power Flow (D-OPF): Modelling, Analysis, and Benchmarking," *IEEE Transactions on Power Systems*, vol. 38, no. 4, pp. 3654-3668, 2022. [[CrossRef](#)] [[Google Scholar](#)] [[Publisher Link](#)]
- [19] Shin-Yeu Lin, and Jyun-Fu Chen, "Distributed Optimal Power Flow for Smart Grid Transmission System with Renewable Energy Sources," *Energy*, vol. 56, pp. 184-192, 2013. [[CrossRef](#)] [[Google Scholar](#)] [[Publisher Link](#)]
- [20] Satish Kansal, Vishal Kumar, and Barjeev Tyagi, "Optimal Placement of Different Types of DG Sources in Distribution Networks," *Electric Power Energy Systems*, vol. 53, pp. 752-760, 2013. [[CrossRef](#)] [[Google Scholar](#)] [[Publisher Link](#)]
- [21] Masoud Esmaili, "Placement of Minimum Distributed Generation Units Observing Power Losses and Voltage Stability with Network Constraints," *IET Generation, Transmission & Distribution*, vol. 7, pp. 813-821, 2013. [[CrossRef](#)] [[Google Scholar](#)] [[Publisher Link](#)]
- [22] M.H. Moradi, and M. Abedini, "A Combination of Genetic Algorithm and Particle Swarm Optimization for Optimal DG Location and Sizing in Distribution Systems," *International Journal of Electrical Power & Energy Systems*, vol. 34, no. 1, pp. 66-74, 2012. [[CrossRef](#)] [[Google Scholar](#)] [[Publisher Link](#)]
- [23] Ridha Djamel Mohammedi et al., "Optimal DG Placement and Sizing in Radial Distribution Systems using NSGA-II for Power Loss Minimization and Voltage Stability Enhancement," *International Review of Electrical Engineering (IREE)*, vol. 8, no. 6, pp. 1806-1814, 2013. [[Google Scholar](#)] [[Publisher Link](#)]
- [24] Henrik Bjørnebye, Cathrine Hagem, and Arne Lind, "Optimal Location of Renewable Energy," *Energy*, vol. 147, pp. 1203-1215, 2018. [[CrossRef](#)] [[Google Scholar](#)] [[Publisher Link](#)]
- [25] Kanchan Jha, and Abdul Gafoor Shaik, "A Comprehensive Review of Power Quality Mitigation in the Scenario of Solar PV Integration into Utility Grid," *e-Prime - Advances in Electrical Engineering, Electronics and Energy*, vol. 3, pp. 1-18, 2023. [[CrossRef](#)] [[Google Scholar](#)] [[Publisher Link](#)]
- [26] Lue Xiong, Mutasim Nour, and Eyad Radwan, "Harmonic Analysis of Photovoltaic Generation in Distribution Network and Design of Adaptive Filter," *International Journal of Computing and Digital Systems*, vol. 9, no. 1, pp. 77-85, 2020. [[CrossRef](#)] [[Google Scholar](#)] [[Publisher Link](#)]
- [27] Kitmo, Guy Bertrand Tchaya, and Noël Djongyang, "Optimisation of Photovoltaic Systems on the Interconnected Electricity Grid in Northern Cameroon-A Review," *International Journal of Energy and Environmental Engineering*, vol. 13, no. 1, pp. 305-317, 2022. [[CrossRef](#)] [[Google Scholar](#)] [[Publisher Link](#)]
- [28] Om Prakash Mahela et al., "Harmonic Mitigation and Power Quality Improvement in the Electricity Grid with Solar Energy Penetration using a Static Distribution Compensator," *IET Power Electronics*, vol. 14, no. 5, pp. 912-922, 2021. [[CrossRef](#)] [[Google Scholar](#)] [[Publisher Link](#)]
- [29] Hadi Saadat, *Power System Analysis*, 3<sup>rd</sup> ed., PSA Publishing, North York, USA, 2010. [[Google Scholar](#)]
- [30] F. Fissou Amigue et al., "Optimal Integration of Photovoltaic Power into the Electricity Network using Slime Mould Algorithms: Application to the Interconnected Grid in North Cameroon," *Energy Reports*, vol. 7, pp. 6292-6307, 2021. [[CrossRef](#)] [[Google Scholar](#)] [[Publisher Link](#)]
- [31] Mohamed Zellagui et al., "Multi-Objective Optimal Allocation of Hybrid Photovoltaic Distributed Generators and Distribution Static Var Compensators in Radial Distribution Systems using Various Optimisation Algorithms," *Journal of Electrical System*, vol. 18, no. 1, pp. 1-22, 2022. [[CrossRef](#)] [[Google Scholar](#)] [[Publisher Link](#)]
- [32] S. Pawar, and M. History, "Harmonic Analysis of High Penetration PV System on Distribution Network," *International Journal of Applied Engineering Research*, vol. 6, no. 6, pp. 401-408, 2019. [[Google Scholar](#)]
- [33] Ali A. Chowdhury, Sudhir K. Agarwal, and D.O. Koval, "Modelling the Reliability of Distributed Generation in the Planning and Analysis of Conventional Distribution Systems," *IEEE Transactions on Industry Applications*, vol. 39, no. 5, pp. 1493-1498, 2003. [[CrossRef](#)] [[Google Scholar](#)] [[Publisher Link](#)]
- [34] Eligius M.T. Hendrix, and Boglárka G.-Tóth, *Introduction to Nonlinear and Global Optimisation*, 1<sup>st</sup> ed., Springer, vol. 37, 2010. [[Google Scholar](#)] [[Publisher Link](#)]
- [35] Daniel Pál et al., "Optimisation of Active Power Losses in Smart Grids using Photovoltaic Power Plants," *Energies*, vol. 15, no. 3, pp. 1-14, 2022. [[CrossRef](#)] [[Google Scholar](#)] [[Publisher Link](#)]
- [36] Kitmo et al., "Optimisation of Power Flow from Photovoltaic Generators in Electrical Networks using the MPPT Algorithm and Parallel Active Filters," *Energy Reports*, vol. 7, supplement 5, pp. 491-505, 2021. [[CrossRef](#)] [[Google Scholar](#)] [[Publisher Link](#)]
- [37] Aslam A Ahmed et al., "NEPLAN-Based Analysis of the Impacts of Electric Vehicle Charging Strategies on the Electricity Distribution System," *IOP Conference Series: Materials Science and Engineering, International Scientific Forum (ISF 2019)*, Malacca, Malaysia, vol. 1127, no. 1, pp. 1-15, 2021. [[CrossRef](#)] [[Google Scholar](#)] [[Publisher Link](#)]
- [38] Kim-Hung Pho, "Improvements to the Newton-Raphson Method," *Journal of Computational and Applied Mathematics*, vol. 408, 2022. [[CrossRef](#)] [[Google Scholar](#)] [[Publisher Link](#)]